

7-2017

Current-driven interface magnetic transition in complex oxide heterostructure

F. Fang

College of William and Mary

H. Zhai

College of William and Mary

X. Ma

College of William and Mary, xma@email.wm.edu

Y. W. Yin

Qi Li

See next page for additional authors

Follow this and additional works at: <https://scholarworks.wm.edu/aspubs>

Recommended Citation

Fang, F.; Zhai, H.; Ma, X.; Yin, Y. W.; Li, Qi; and Lupke, G., Current-driven interface magnetic transition in complex oxide heterostructure (2017). *JOURNAL OF VACUUM SCIENCE & TECHNOLOGY B*, 35(4).
10.1116/1.4976587

This Article is brought to you for free and open access by the Arts and Sciences at W&M ScholarWorks. It has been accepted for inclusion in Arts & Sciences Publications by an authorized administrator of W&M ScholarWorks. For more information, please contact scholarworks@wm.edu.

Authors

F. Fang, H. Zhai, X. Ma, Y. W. Yin, Qi Li, and G. Lupke

Current-driven interface magnetic transition in complex oxide heterostructure

F. Fang, H. Zhai, X. Ma, Y. W. Yin, Qi Li, and G. Lüpke

Citation: *Journal of Vacuum Science & Technology B* **35**, 04F101 (2017); doi: 10.1116/1.4976587

View online: <https://doi.org/10.1116/1.4976587>

View Table of Contents: <http://avs.scitation.org/toc/jvb/35/4>

Published by the [American Vacuum Society](#)

Articles you may be interested in

[Role of neutral transport in aspect ratio dependent plasma etching of three-dimensional features](#)

Journal of Vacuum Science & Technology A: Vacuum, Surfaces, and Films **35**, 05C301 (2017); 10.1116/1.4973953

[Interface magnetization transition via minority spin injection](#)

Applied Physics Letters **109**, 232903 (2016); 10.1063/1.4972035

[Flexible InP based quantum dot light-emitting diodes using Ag nanowire-colorless polyimide composite electrode](#)

Journal of Vacuum Science & Technology B, Nanotechnology and Microelectronics: Materials, Processing, Measurement, and Phenomena **35**, 04E101 (2017); 10.1116/1.4984804

[Creating and probing quantum dot molecules with the scanning tunneling microscope](#)

Journal of Vacuum Science & Technology B, Nanotechnology and Microelectronics: Materials, Processing, Measurement, and Phenomena **35**, 04F102 (2017); 10.1116/1.4979848

[Theoretical investigations on the stability and electronic structures of two-dimensional group-IV ternary alloy monolayers](#)

Journal of Vacuum Science & Technology B, Nanotechnology and Microelectronics: Materials, Processing, Measurement, and Phenomena **35**, 04F103 (2017); 10.1116/1.4980048

[Review Article: Flow battery systems with solid electroactive materials](#)

Journal of Vacuum Science & Technology B, Nanotechnology and Microelectronics: Materials, Processing, Measurement, and Phenomena **35**, 040801 (2017); 10.1116/1.4983210



Instruments for Advanced Science

Contact Hiden Analytical for further details:
www.HidenAnalytical.com
info@hiden.co.uk

CLICK TO VIEW our product catalogue



Gas Analysis

- dynamic measurement of reaction gas streams
- catalysis and thermal analysis
- molecular beam studies
- dissolved species probes
- fermentation, environmental and ecological studies



Surface Science

- UHV TPD
- SIMS
- end point detection in ion beam etch
- elemental imaging - surface mapping



Plasma Diagnostics

- plasma source characterization
- etch and deposition process reaction kinetic studies
- analysis of neutral and radical species



Vacuum Analysis

- partial pressure measurement and control of process gases
- reactive sputter process control
- vacuum diagnostics
- vacuum coating process monitoring

Current-driven interface magnetic transition in complex oxide heterostructure

F. Fang, H. Zhai, and X. Ma

Department of Applied Science, College of William & Mary, Williamsburg, Virginia 23187

Y. W. Yin and Qi Li

Department of Physics, Pennsylvania State University, University Park, Pennsylvania 16802

G. Lüpke^{a)}

Department of Applied Science, College of William & Mary, Williamsburg, Virginia 23187

(Received 22 December 2016; accepted 31 January 2017; published 16 February 2017)

The interfacial spin state of n-type BaTiO₃/La_{0.5}Ca_{0.5}MnO₃/La_{0.7}Sr_{0.3}MnO₃ heterojunction and its dependence on gate voltage is investigated with magnetic second-harmonic generation at 78 K. The injection of minority spins alters the interface magnetization of La_{0.7}Sr_{0.3}MnO₃ from ferromagnetic to antiferromagnetic exchange coupled, while the bulk magnetization remains unchanged. The emergent interfacial antiferromagnetic interactions are attributed to modulations of the strong double-exchange interaction between conducting electron spins and local magnetic moments. The results will help promote the development of new interface-based functionalities and device concepts.

© 2017 American Vacuum Society. [<http://dx.doi.org/10.1116/1.4976587>]

I. INTRODUCTION

Electrical control of magnetism is a key issue for future development of low-power spintronics and magnetic random access memories.^{1–3} In multiferroic tunnel junctions, the magnetoelectric (ME) response enables the interfacial magnetization to be manipulated by an electric field through switching of the ferroelectric (FE) polarization resulting in a four-state resistance and large tunneling electroresistance effect.^{4–13} The so-called *magnetoelectric interfaces* present a novel route toward using the spin degree of freedom in electronic devices.^{14,15} This route is carried out by fabricating well-defined interfaces between transition metal oxides, to engineer and cross-couple their unique electric, magnetic, and transport properties.^{16,17} A good candidate for the magnetic constituent of such interface is doped manganite, which received detailed understanding on carrier filling and orbital effects.^{18,19} To realize electronic and structural reconstructions of doped manganite, electrostatic and strain effects are primary methods, which modulate the competition between different interactions.^{14,15}

Recently, researchers successfully employed polarized FE layers, e.g., Pb(Zr_{0.2}Ti_{0.8})O₃ (PZT) or BaTiO₃ (BTO), to alter the magnetic state at the interface of the ferromagnetic (FM) La_{0.7}Sr_{0.3}MnO₃ (LSMO) layer.^{20,21} Moreover, Yin *et al.* observed a giant tunneling electroresistance ratio of ~3300% by inserting a 1-nm thick La_{0.5}Ca_{0.5}MnO₃ (LCMO) barrier in the junction of LSMO/BTO/LSMO.²² The results suggest a ferroelectrically induced metal-insulator phase transition in the LCMO layer that is of ME origin. This has been investigated by Yi *et al.*,²³ who observed direct evidence for a ferromagnetic-to-antiferromagnetic (AFM) state transition in LCMO controlled by the FE polarization of BiFeO₃. The interfacial ME coupling effect is mainly derived from the superexchange between Mn and Fe *t*_{2g}

spins.²³ The authors also suggest that there may be similar pathways to implement a reversible switch between FM and AFM states.²³ In this study, we report on a current-induced ME effect that alters the interface magnetization of BTO/LCMO/LSMO heterojunction.

II. EXPERIMENTAL RESULTS

Here, we use magnetic second-harmonic generation (MSHG) to selectively probe the interface magnetization of complex oxide heterostructures as a function of gate voltage U_g [Fig. 1(a)]. We fabricated indium-tin-oxide (ITO)(50 nm)/BTO(100 nm)/LCMO(1 nm)/LSMO (50 nm) and ITO(50 nm)/BTO(200 nm)/LSMO(50 nm) heterostructures epitaxially grown on SrTiO₃ (STO) substrates by pulsed laser deposition. The ITO and LSMO layer serve as top and bottom electrodes, respectively [Fig. 1(a)]. We refer to these heterojunctions as samples J1 and J2, respectively. The interfaces of the perovskite layers were characterized on a control sample by scanning transmission electron microscopy with aberration correction and low-loss electron energy loss spectroscopy.²² The MSHG technique is well suited for probing the interfacial magnetic state where both spatial-inversion and time-reversal symmetries are broken.^{21,24–26} For comparison, magneto-optical Kerr effect (MOKE) measurements are employed to detect the bulk magnetization. All measurements are performed at 78 K.

Figures 1(b) and 1(c) display the interfacial and bulk magnetization loops of the BTO/LCMO/LSMO heterostructure (J1) as a function of gate voltage probed with MSHG and MOKE, respectively. The key findings are twofold: (1) the interface magnetization is modulated by the applied voltage, while the bulk magnetization is not; and (2) both interface and bulk hysteresis loops are similar with a coercive field $H_c \sim 40$ Oe. The result suggests that the magnetization of LSMO at the heterointerface is altered with different gate voltages while the magnetic state of bulk LSMO does not

^{a)}Electronic mail: luepke@wm.edu

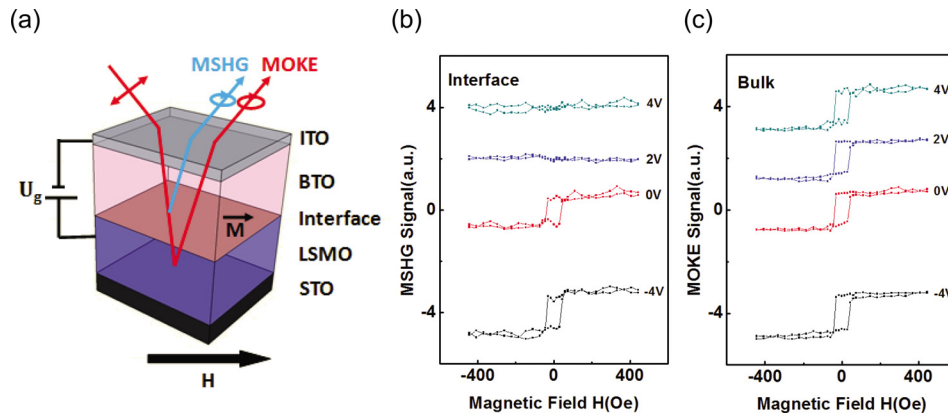


FIG. 1. (Color online) (a) Schematic depiction of MSHG and MOKE measurement—MOKE measures the bulk magnetization of the LSMO film, while MSHG selectively probes the interface magnetization only. (b) Interface and (c) bulk magnetic hysteresis loops from BTO/LCMO/LSMO heterostructure (J1) for different external gate voltages U_g measured with MSHG and MOKE techniques at 78 K, respectively.

change. The observation is consistent with MSHG and MOKE loops obtained from the BTO/LSMO heterostructure (J2).²⁵ In what follows, we attribute the change of MSHG signal to minority spin injection and accumulation at the heterointerface, resulting in a change of magnetic ordering of interfacial Mn ions in LSMO.

Next, we discuss the change of interface magnetization as a function of U_g in terms of the magnetic contrast of the MSHG loop [Fig. 2(a)]. The magnetic contrast for a hysteresis loop is defined as²¹

$$A = \frac{I(+M) - I(-M)}{I(+M) + I(-M)}, \quad (1)$$

where $I(+M)$ and $I(-M)$ are the intensities for the two magnetization states. The magnetic contrast A can be understood as the height of the jump in the hysteresis loop divided by the sum of the intensities of both magnetizations. Figure 2(a) displays the magnetic contrast A obtained from the MSHG hysteresis loops of sample J1 as a function of U_g , as shown in Fig. 1(b). For $U_g < +1$ V, the interfacial LSMO is in the FM state since the magnetic contrast is obvious. Above +1 V, the magnetic contrast A suddenly vanishes, indicating a magnetic transition to AFM phase since a paramagnetic phase is unlikely to occur in LSMO at 78 K due to the strong superexchange interaction of t_{2g} electrons of neighboring Mn ions. We attribute this sudden, reversible FM-to-AFM state transition to an interface ME effect.

Figure 2(b) displays the I-V curve obtained from sample J1, which clearly shows rectifying behavior with an onset of current flow across the heterojunction at positive U_g . This indicates that the observed interface magnetic transition occurs near the flatband voltage, and hence, it is not driven by the electric field at the heterojunction. Furthermore, the P-V curve [Fig. 2(b), inset] shows that the observed interface magnetic transition is not caused by polarization switching of the BTO layer. There is no sudden jump in the P-V curve nor does the magnetic contrast A exhibit a hysteresis loop. The observed interface ME effect is therefore not related to the electrostatic charge-induced interface magnetic transition of LSMO, as observed for PZT/LSMO

interface.^{20,21} This points toward a new mechanism for the observed interface ME coupling effect in the LSMO layer, caused by the forward current through the junction. The magnetic properties of the ultrathin LCMO interlayer are not observed or distinguished, as it is initially AFM at zero gate voltage and can be tuned to other states by different carrier injection (a special kind of doping).²²

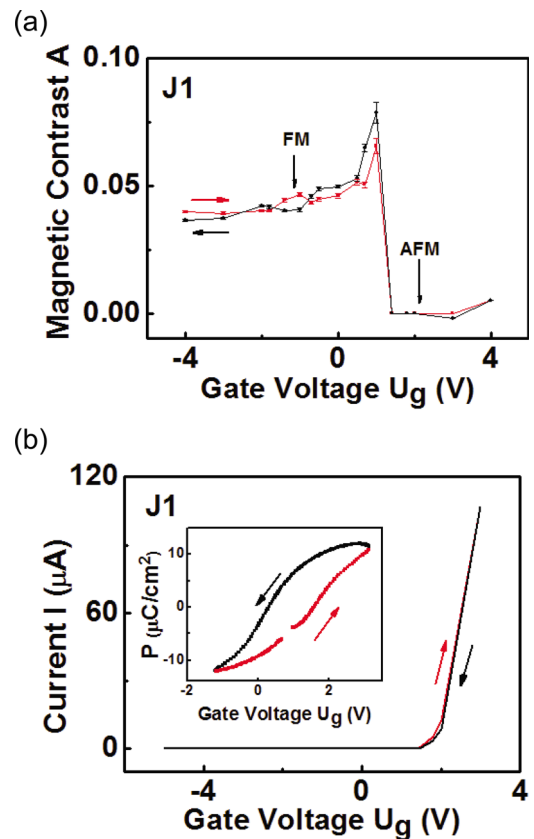


FIG. 2. (Color online) (a) MSHG magnetic contrast A as a function of gate voltage U_g from BTO/LCMO/LSMO heterostructure (J1). (b) I-V curve measured from sample J1 at 78 K. Decreasing (increasing) gate voltages are labeled in black (red). The inset shows the ferroelectric polarization (P) in BTO as a function of U_g measured at 78 K. The direction of positive P is defined as pointing away from LSMO electrode.

III. DISCUSSION

Next, we discuss the microscopic mechanism of the observed interface ME effect. Figure 3 shows a schematic of the proposed magnetic structure and spin alignment at the BTO/LCMO/LSMO heterojunction. For simplicity, the LCMO interlayer is not shown. For FE polarization pointing away from the LSMO layer, the hole accumulation biases the interfacial LSMO layer toward the AFM insulating phase. However, the $\text{La}_{0.7}\text{Sr}_{0.3}\text{MnO}_3$ has stoichiometry that is far enough from the phase boundary and a change in magnetic order is not expected owing to a build-up of screening charge.²² On the other hand, for a positive gate voltage applied to the LSMO layer [Fig. 3(b)], an electron current begins to flow through the BTO/LSMO heterojunction. Both, spin-up and spin-down electrons will be injected from the conduction band of BTO into the interfacial LSMO layer, since the spin polarization of LSMO surfaces extracted from transport measurements usually yield less than 95%.²⁷ The majority spin-up electrons will quickly relax to the Fermi level and conduct through the LSMO layer. In contrast, the minority spin-down electrons will strongly interact with the local spins of the t_{2g} electrons due to the large Hund's rule coupling. This will weaken the double-exchange mechanism and hence reduce the ferromagnetic coupling between Mn

ions at the LSMO interface. At a critical gate voltage U_c , the injected minority spin-down electrons will reduce the double-exchange mechanism such that the super-exchange interaction will dominate, and the interfacial LSMO layer will undergo a FM-to-AFM state transition. This magnetic reconstruction will occur in a few Mn layers at the interface since the minority spin-down electrons will strongly scatter with electrons, phonons, and magnons, resulting in spin-flip processes.²⁸ The primary one is the Elliott-Yafet-type of spin-flip scattering, which usually takes place on a time scale of a few hundred femtoseconds.²⁹ For comparison, the characteristic timescales of double- and super-exchange coupling, $J \approx -10$ and 7 K ,³⁰ can be estimated via Heisenberg relation $\tau = \hbar/|J| \approx 4\text{ ps}$. The magnetic reconstruction at the interface also leads to spin frustration, with the competition between AFM coupling at the interface and FM ground state of bulk LSMO. To achieve a more energetically favorable state, the spins in the interfacial layer will cant along the spin direction of the bulk LSMO.

We may speculate about the orbital/spin ordering in the interfacial LSMO layer. If the $d_{3z^2-r^2}$ orbitals are energetically favored, then the double-exchange interaction induced by hopping of e_g electrons is stronger in the z direction (surface normal), while super-exchange coupling induced

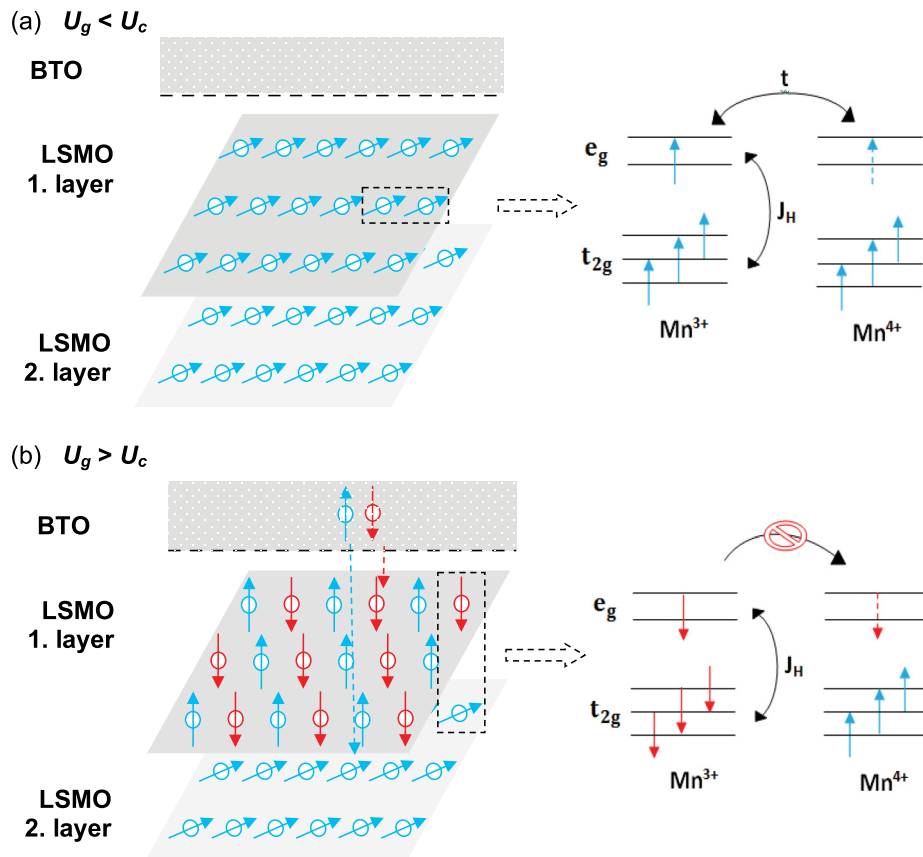


FIG. 3. (Color online) (a) Below critical gate voltage U_c , majority spins (up arrows) of Mn^{3+} and Mn^{4+} ions are double-exchange coupled (right panel), leading to a ferromagnetic state of LSMO. (b) Above U_c , majority spins flow across the LSMO layer by spin-hopping process t . In contrast, the minority spins (down arrows) will accumulate at the interface, since the spin-hopping process t is blocked by the strong interaction with the local spins due to the large Hund's rule coupling J_H (right panel). The AFM super-exchange interaction of t_{2g} electrons between neighboring Mn ions dominates, and the interfacial LSMO layer undergoes a FM-to-AFM phase transition.

by local t_{2g} electrons is stronger in the x - y plane (surface plane). This interfacial $d_{3z^2-r^2}$ orbital occupation favors the C-type AFM spin ordering, and the easy axis of the AFM phase is oriented along z direction.³¹ This orbital/spin ordering is consistent with our observation that the MSHG magnetic contrast vanishes as the spin coupling on x - y plane is tuned into AFM type at the LSMO interface. On the other hand, the $d_{x^2-y^2}$ ordering naturally leads to the AFM coupling between adjacent Mn layers via the superexchange interaction, which is responsible for the A-type (planar) AFM ordering in LSMO. This would not cause the MSHG magnetic contrast to vanish, if the MSHG signal is generated in the first Mn layer at the interface. These observations are consistent with our recent findings from n-type BTO/LSMO (Ref. 25) and n-type STO/LCMO/LSMO (Ref. 26) heterostructures, where the injection of minority spins at the interface causes a sudden, reversible transition of the spin alignment of interfacial Mn ions from ferromagnetic to C-type antiferromagnetic exchange coupled. We note, that the ultrathin LCMO interlayer improves significantly the MSHG magnetic contrast in these complex oxide heterostructures, which is consistent with the observation by Yin *et al.* of a much enhanced tunneling electroresistance ratio of $\sim 3300\%$ by inserting a 1-nm thick LCMO barrier in the junction of LSMO/BTO/LSMO.²² On the other hand, this study shows that the critical gate voltage U_c of the interface magnetic transition does not depend strongly on the LCMO interlayer.

IV. CONCLUSION

The observed current-induced interfacial magnetoelectric coupling mechanism is conceptually different from those known previously, such as FE polarization-induced changes in the lattice strain or nature of chemical bonding, and/or charge (carrier) modulation at the multiferroic heterojunction.¹⁵ Both can affect the FM moments at the interface of a LSMO or LCMO layer, as expected from their critical phase-competitive nature in magnetism. Here, the injected minority spins through strong Hund's interaction with the local magnetic moments cause a sudden and reversible magnetic transition at the LSMO interface. The results are important for the transport properties of magnetic tunneling junctions, because an interfacial magnetic transition may notably change the spin polarization of the tunneling current and thus be decisive for tunneling magnetoresistance.

ACKNOWLEDGMENTS

The MSHG experiments, data analysis, and discussions performed at College of William and Mary were supported by the Department of Energy (Grant No. DE-FG02-04ER46127). The work at Pennsylvania State University (PSU) was supported in part by the DOE (Grant No. DE-FG02-08ER4653) and the NSF (Grant No. DMR-1207474).

- ¹F. Matsukura, Y. Tokura, and H. Ohno, *Nat. Nanotechnol.* **10**, 209 (2015).
- ²R. Ramesh, *Nat. Mater.* **9**, 380 (2010).
- ³W. Eerenstein, N. D. Mathur, and J. F. Scott, *Nature* **442**, 759 (2006).
- ⁴E. Y. Tsymbal and H. Kohlstedt, *Science* **313**, 181 (2006).
- ⁵C.-G. Duan, S. S. Jaswal, and E. Y. Tsymbal, *Phys. Rev. Lett.* **97**, 047201 (2006).
- ⁶M. Gajek, M. Bibes, S. Fusil, K. Bouzehouane, J. Fontcuberta, A. Barthélémy, and A. Fert, *Nat. Mater.* **6**, 296 (2007).
- ⁷J. F. Scott, *Nat. Mater.* **6**, 256 (2007).
- ⁸J. P. Velev, C.-G. Duan, J. D. Burton, A. Smogunov, M. K. Niranjan, E. Tosatti, S. S. Jaswal, and E. Y. Tsymbal, *Nano Lett.* **9**, 427 (2009).
- ⁹V. Garcia *et al.*, *Science* **327**, 1106 (2010).
- ¹⁰M. Hambe, A. Petraru, N. A. Pertsev, P. Munroe, V. Nagarajan, and H. Kohlstedt, *Adv. Funct. Mater.* **20**, 2436 (2010).
- ¹¹Y. W. Yin, M. Raju, W. J. Hu, X. J. Weng, X. G. Li, and Q. Li, *J. Appl. Phys.* **109**, 07D915 (2011).
- ¹²D. Pantel, S. Goetze, D. Hesse, and M. Alexe, *Nat. Mater.* **11**, 289 (2012).
- ¹³Y. W. Yin, M. Raju, W. J. Hu, X. J. Weng, K. Zou, J. Zhu, X. G. Li, Z. D. Zhang, and Q. Li, *Front. Phys.* **7**, 380 (2012).
- ¹⁴J. D. Burton and E. Y. Tsymbal, *Philos. Trans. R. Soc. A* **370**, 4840 (2012).
- ¹⁵C. A. F. Vaz, F. J. Walker, C. H. Ahn, and S. Ismail-Beigi, *J. Phys.: Condens. Matter* **27**, 123001 (2015).
- ¹⁶Y. Tokura and H. Y. Hwang, *Nat. Mater.* **7**, 694 (2008).
- ¹⁷J. Mannhart and D. G. Schlom, *Science* **327**, 1607 (2010).
- ¹⁸Y. Tokura and N. Nagaosa, *Science* **288**, 462 (2000).
- ¹⁹I. V. Solovyev and K. Terakura, *Phys. Rev. Lett.* **82**, 2959 (1999).
- ²⁰C. A. F. Vaz, J. Hoffman, Y. Segal, J. W. Reiner, R. D. Grober, Z. Zhang, C. H. Ahn, and F. J. Walker, *Phys. Rev. Lett.* **104**, 127202 (2010).
- ²¹X. Ma, A. Kumar, S. Dussan, H. Zhai, F. Fang, H. B. Zhao, J. F. Scott, R. S. Katiyar, and G. Lüpke, *Appl. Phys. Lett.* **104**, 132905 (2014).
- ²²Y. W. Yin *et al.*, *Nat. Mater.* **12**, 397 (2013).
- ²³D. Yi, J. Liu, S. Okamoto, S. Jagannatha, Y.-C. Chen, P. Yu, Y.-H. Chu, E. Arenholz, and R. Ramesh, *Phys. Rev. Lett.* **111**, 127601 (2013).
- ²⁴Y. Fan, K. J. Smith, G. Lüpke, A. T. Hanbicki, R. Goswami, C. H. Li, H. B. Zhao, and B. T. Jonker, *Nat. Nanotechnol.* **8**, 438 (2013).
- ²⁵F. Fang, H. Zhai, X. Ma, Y. W. Yin, Q. Li, and G. Lüpke, *Appl. Phys. Lett.* **109**, 232903 (2016).
- ²⁶F. Fang, Y. W. Yin, Q. Li, and G. Lüpke, *Sci. Rep.* **7**, 40048 (2017).
- ²⁷M. Bowen, M. Bibes, A. Barthélémy, J.-P. Contour, A. Anane, Y. Lemaître, and A. Fert, *Appl. Phys. Lett.* **82**, 233 (2003).
- ²⁸K. G. Rana, T. Yajima, S. Parui, A. F. Kemper, T. P. Devereaux, Y. Hikita, H. Y. Hwang, and T. Banerjee, *Sci. Rep.* **3**, 1274 (2013).
- ²⁹M. Cinchetti *et al.*, *Phys. Rev. Lett.* **97**, 177201 (2006).
- ³⁰P. Fazekas, *Lecture Notes on Electron Correlation and Magnetism* (World Scientific, Singapore, 1999), p. 231.
- ³¹C. Aruta, G. Ghiringhelli, V. Bisogni, L. Braicovich, N. B. Brookes, A. Tebano, and G. Balestrino, *Phys. Rev. B* **80**, 014431 (2009).